Swelling as a promoter of migration of plastic additives in the interaction of fatty food simulants with polylactic acid- and polypropylene-based plastics

Kirchkeszner Cs., Petrovics N., Tábi T., Magyar N., Kovács J., Szabó B. S., Nyiri Z., Eke Zs.

Swelling as a promoter of migration of plastic additives in the interaction of fatty food simulants with polylactic acid- and polypropylene-based plastics

Csaba Kirchkeszner[a,b,‡], Noémi Petrovics[a,b, ‡], Tamás Tábi[c,d], Norbert Magyar[e], József Kovács[f], Bálint Sámuel Szabó[a,b], Zoltán Nyiri[b], Zsuzsanna Eke[a,g*]

[a] Hevesy György PhD School of Chemistry, Eötvös Loránd University, Pázmány Péter stny. 1/A, H-1117 Budapest, Hungary

[b] Joint Research and Training Laboratory on Separation Techniques, Institute of Chemistry, Eötvös Loránd University, Pázmány Péter stny. 1/A, H-1117 Budapest, Hungary

[c] Department of Polymer Engineering, Faculty of Mechanical Engineering, Budapest University of Technology and Economics, Műegyetem rkp. 3, H-1111 Budapest, Hungary

[d] MTA-BME Research Group for Composite Science and Technology, Műegyetem rkp. 3, H-1111 Budapest, Hungary

[e] Department of Methodology for Business Analyses, Faculty of Commerce, Hospitality and Tourism, Budapest Business School, Alkotmány u. 9–11, H-1054 Budapest, Hungary

[f] Department of Geology, Institute of Geography and Earth Sciences, Eötvös Loránd University, Pázmány Péter stny. 1/C, H-1117 Budapest, Hungary

[g] Wessling International Research and Educational Center, Anonymus u. 6, H-1045 Budapest, Hungary

* Corresponding author. E-mail address: zsuzsanna.eke@ttk.elte.hu (Zsuzsanna Eke)
Phone number: +36-30-598-0300

‡ These two authors contributed equally to the work.

E-mail addresses: csaba.kirchkeszner@ekol.chem.elte.hu, noemi.petrovics@ekol.chem.elte.hu, tabi@pt.bme.hu, magyar.norbert@uni-bge.hu, kevesolt@geology.elte.hu, balint.szabo@ekol.chem.elte.hu, zoltan.nyiri@ekol.chem.elte.hu

Abstract

The migration of various plastic additives (antioxidants: BHT, Ionox 220, Irgafos 168; UV absorber: Uvinul 3039; plasticizers: TBAC and TOTM) from polypropylene and polylactic acid was investigated in a series of experiments conducted over a period of 13 days. As fatty food simulants, both ethanol 95 *v*/*v*% and isooctane were used. Non-Fickian behaviour was observed on multiple occasions. The kinetic curves of both migration concentrations and swelling were evaluated using variography to determine objectively the starting points of long-lasting plateaus as well as short halts in the increase. A strong correlation between migration and swelling was observed: the kinetic curves showed that migration always followed swelling. Also, more intensive swelling results in the increased migration of the additivies. Consequently, migration testing can be improved by considering the swelling of the plastic.

Keywords

polylactic acid (PLA), polypropylene (PP), food contact materials (FCM), migration kinetics, swelling effect, variography

Highlights

- Migration and swelling kinetics of polylactic acid and polypropylene were studied.
- Swelling strongly affects plastic additive migration from food contact materials.
- The effect of molecular weight on additive migration can be overruled by plasticizers.
- Variography was successfully applied to identify steady-states on kinetic curves.

1. Introduction

Plastic food contact materials (FCPs) play an indispensable role in food production, storage, transport and safety. Nowadays, the most commonly used FCPs are petrochemical-based polymers, such as polyethylene (PE) and polypropylene (PP). Its low price, good malleability, and strong water barrier properties make PP a remarkable raw material in the manufacture of food packaging. However, the rapid growth of environmental awareness has increased demand for the use of biodegradable polymers. For food industry applications, the most prominent biopolymer is polylactic acid (PLA), due to its high mechanical strength, good optical properties, low toxicity, and relatively low price.

Along with polymers, FCPs also contain additives; antioxidants, UV stabilizers, slip agents, nucleating agents, plasticizers and various other additives are used to prevent the degradation of plastic products and improve the processability of the raw material. These chemical compounds and their contaminants or degradation products can migrate from the FCP into the food, which might pose a serious risk to human health. Migration studies are therefore required in the case of plastic materials that are to be used as food contact materials. Commission Regulation (EU) 10/2011 of 14 January 2011 on "Plastic materials and articles intended to come into contact with food" **(Commission Regulation (EU) 10/2011, 2011)** lays down rules for the basic circumstances (e.g. contact time, temperature) of such tests. Some standard test settings are also determined, e.g. long-term storage at room temperature or below are to be modelled using a 10 day migration test at elevated temperatures (40 °C or 60 °C).

Furthermore, the use of six food simulants instead of real food is prescribed. The choice of appropriate simulant depends on the characteristics of the food intended to come into contact with the FCP. For instance, vegetable oil with less than 1% unsaponifiable matter is specified as a substitute for lipophilic food **(Commission Regulation (EU) 10/2011, 2011)**. Nevertheless, this food simulant is rarely used in specific migration studies, since it is not compatible with either gas (GC) or reversed-phase high-performance liquid chromatographic (RP-HPLC) analytical systems. Usually, 2,2,4-trimethylpentane (isooctane) and ethanol 95 *v*/*v*% are used instead **(Aznar et al., 2019; Garde et al., 2001; Lu et al., 2021; Ramos et al., 2014; Vera et al., 2018; Yang et al., 2016)**. These are the solvents also specified in the current consolidated version of the aforementioned regulation **(Commission Regulation (EU) 10/2011, 2011)** for cases when it is not technically feasible to work with vegetable oil. For such cases, however, the use of both solvents is required. With this approach, the analytical work becomes incomparably easier, even though it duplicates the number of samples to be analyzed. In the end, to ensure consumer safety, any decision on compliance of the FCP tested must be based on the highest observed concentrations. This means the number of samples to be analyzed can be kept under control if the solvent providing a more intensive migration is known prior to the testing.

Migration is a complex process, the result of diffusion, dissolution, and equilibrium (**Manzanarez-López et al., 2011; Samsudin et al., 2018**). Therefore, a deeper understanding of this phenomenon is based on kinetic tests, in which the time dependence of mass transfer is investigated. Several kinetic studies on the migration of various compounds into food simulants are available. These studies usually aim at demonstrating the applicability of the tested compounds to become the active agent of active packaging and thus focus on the release of antioxidants **(Chang et al., 2019; Garde et al., 2001; Jamshidian et al., 2012, 2013; Kang et al., 2018; Manzanarez-López et al., 2011; Ramos et al., 2014)** or antimicrobial compounds **(Kuorwel et al., 2013; Mascheroni et al., 2010)** from thin plastic films (typically 50–200 μm). Recently, **Kang et al. (2018)** investigated concentrations of BHT and Irganox 1010 in food simulants migrating from PP after pre-treatments mimicking severe food processing conditions, such as sterilization at 121 °C, microwave cooking, and deep freezing. The concentrations observed were presented as a function of contact time, thus demonstrating how the conditions under consideration can amplify migration. A more widespread approach is to assume that Fick's second law of diffusion applies and calculate diffusion coefficients by determining the correlation between migrated concentrations (M_t) normalized with migrated concentration at equilibrium (M_∞) and contact time (t) **(Chang et al., 2019; Garde et al., 2001; Gavriil et al., 2018; Jamshidian et al., 2012, 2013; Kuorwel et al., 2013; Manzanarez-López et al., 2011; Mascheroni et al., 2010; Ramos et al., 2014)**.

However, non-Fickian behaviour has been reported on multiple occasions. In a study on the release of α-tocopherol from PLA films (α-tocopherol content: 2.58 *w%*) to oil and ethanol, **Manzanerez-López et al. (2011)** observed an apparent equilibrium at 73 hours in ethanol at 33 °C. After 106 hours of contact, the concentration of α-tocopherol in the ethanol phase started to increase again, reaching a new equilibrium at 269 hours. Apparent equilibrium was also found by **Iñiguez-Franco et al. (2012)**, in the case of catechin and epicatechin migration from PLA (at contact temperatures of 20 °C and 30 °C). **Feigenbaum et al. (2000)** reported that the diffusion coefficient of aromatic antioxidants migrating from PP random copolymer into isooctane increased constantly before the concentration of the antioxidants in the isooctane phase reached a plateau. **Garde et al. (2001)** pointed out that the penetration of *n*-heptane into PP must cause a time dependence in the diffusion coefficient of antioxidants released from the polymer until the mass transfer of the *n*-heptane is completed. The Fickian migration curves observed were explained as being caused by the swelling process being fast compared to the migration of antioxidants. After the swelling process was completed, the diffusion coefficient became constant, and this was the value measured experimentally. **Mascheroni et al. (2010)** applied Fickian models with three different boundary conditions to the prediction of the diffusivity of propolis compounds from PLA films to ethanol and water. The failure of these theoretical models to predict the migration process was attributed to the swelling effect of ethanol.

Bodai et al. (2015) introduced variography into chemometrics. It was used in the evaluation of kinetic curves of the migration of Tinuvin P and Irganox 3114 from high-density polyethylene. In the field of earth and environmental sciences this method has been successfully applied to obtain the necessary sampling frequency in time **(Hatvani et al., 2012; Kovács et al., 2012)** and space **(Hatvani et al., 2018; Hatvani et al., 2014, 2017, 2020; Kern et al., 2020; Trásy et al., 2018)**, in other words, to find the distance –be it in space or time – at which the data are auto-uncorrelated. **Bodai et al. (2015)** demonstrated that the original geostatistical method can be used to determine the time necessary to reach a steady-state in the concentration of plastic additives in food simulants. This indicates the likelihood of its applicability to the assessment of migration curves showing non-Fickian behaviour.

The plasticizing effect of swelling and its effect of promoting on the migration of polymer additives is widely known. It is usual to explain the relatively high diffusion coefficients obtained using food simulants mimicking fatty food by the swelling of the polymer **(Feigenbaum et al., 2000; Nasiri et al., 2016)**. **Samsudin et al. (2014)** observed a large release of astaxanthin from PLA to 95% ethanol and attributed it to disruptions of the microstructure of the PLA film caused by ethanol. In this study, however, the degree of swelling observed in PLA samples was not determined. Greater emphasis was assigned to the swelling of PLA by ethanol by **Iñiguez-Franco et al. (2017)** in their work on the dependence of ethanol sorption by PLA and PLA nanocomposite on ethanol fraction, demonstrating that PLA became more elastic when it was immersed in a solution with a higher ethanol content. Also, the migration of a nanoclay-related surfactant was followed in a 180 day long release study. A connection between the elevated migration rate of surfactant and polymer swelling was assumed in the early stage of release; the time dependence of solvent uptake was not, however, followed. In general, increased migration is often associated with swelling **(Garde**

et al., 2001; Jamshidian et al., 2012; Manzanarez-López et al., 2011; Ramos et al., 2014), the latter is, however, rarely measured, even though swelling renders the assumption of Fickian diffusion invalid.

In this study, the aim was to take a deeper look at the connection between swelling and migration by correlating their kinetic curves using PLA and PP polymers. Both polymers have well-established uses as FCPs, while their physical-chemical properties differ to a remarkable degree. The experiments conducted in the course of this study were designed bearing the compliance testing of FCPs in mind. A timeframe close to 10 days was adhered to, as this is the maximum necessary testing time according to Commission Regulation (EU) 10/2011 **(Commission Regulation (EU) 10/2011, 2011)**. Beside antioxidants (BHT, Ionox 220, Irgafos 168), a UV absorber (Uvinul 3039) and two plasticizers (TBAC, TOTM) were included. These additives not only cover various functionalities, but also differ in molecular weight. To avoid the need for assuming Fickian behaviour the determination of diffusion coefficients was not pursued, and a decision was made to use variography to determine the onset of steady-states.

2. Materials and Methods

2.1. Chemicals and Materials

Ingeo^{TM} Biopolymer 2500HP polylactic acid polymer resin (*D*-lactide content of 0.5 *w%*) was purchased from NatureWorks LLC (Minnetonka, Minnesota, USA). Tipplen H145F polypropylene homopolymer resin was bought from MOL Group (Budapest, Hungary). Both polymer types are suitable for the production of food contact materials.

The polymers were compounded with five different plastic additives. These were BHT (2,6-di-*tert*-butyl-4-methylphenol, CAS: 128-37-0), Ionox 220 (4,4´-methylene-*bis*(2,6-di-*tert*-butylphenol), CAS: 118-82-1), Uvinul 3039 (2-ethylhexyl 2-cyano-3,3-diphenylacrylate, CAS: 6197-30-4), TBAC (tributyl acetyl citrate, CAS: 77-90-7) and TOTM (*tris*(2-ethylhexyl) trimellitate), CAS: 3319-31-1). Besides, the PP resin originally contained the antioxidant Irgafos 168 (*tris*(2,4-di-*tert*-butylphenyl) phosphite, CAS: 31570-04-4) at a concentration of 0.5 *w%*. During sample preparation, mirex (perchloropentacyclodecane, CAS: 2385-85-5) was used as an evaporation standard. BHT, TBAC, TOTM, and mirex were purchased from Sigma-Aldrich Co. (Budapest, Hungary). Ionox 220 was bought from Alfa Aesar (Molar Chemicals, Budapest, Hungary) and the Uvinul 3039 was donated by BASF Hungary Ltd. (Budapest, Hungary).

In the migration tests, isooctane (2,2,4-trimethylpentane, CAS: 54-84-1) and ethanol 95 *v*/*v*% (CAS: 64-17-5) were applied as food simulants of fatty food. HPLC grade isooctane and ethanol were purchased from Thomasker Finechemicals Ltd. (Budapest, Hungary).

The concentration of individual stock solutions of plastic additives and that of mirex were 1000 mg/L and 200 mg/L, respectively. A working solution containing all five additives at 150 mg/L was prepared. Calibration solutions for quantitative analysis were diluted to 10 different concentration levels from the working solution in the 25 μg/L–100 mg/L range. Each solution contained mirex in a concentration of 10 mg/L. Calibration solutions were prepared in both isooctane and ethanol 95 *v*/*v*%. Two linear curves were fitted in each calibration range of target compounds to achieve the appropriate linearity (R^2>0.9900). The lower and upper concentration levels of the calibration linear curves were defined as the lower and upper limits of quantitation (*LLOQ* and *ULOQ*). At these points, recoveries were calculated. *LLOQ* data are listed in ***Table 1***. More detailed information on the calibration curves and representative chromatograms can be found in in ***Supp. Inf. Table 1***.

2.2. Production of Plastic Samples

Plastic specimens were produced in a three-stage technological process. First, the polymer resins were compounded with the additives using a twin-screw extruder. The resulting filaments were then shredded and repelletized. Eventually, square-shaped sheet specimens were made using injection molding.

In the case of PLA, overnight heating at 85 °C was necessary to prevent the hydrolysis of polymer chains during production. In order to avoid possible interference between target compounds and degradation products in quantitative analysis, each polymer was compounded with only one additive. Therefore, the production process resulted in six different types of plastics for both PLA and PP. Additive concentrations were set according to the recommendation of the manufacturers: plastic specimens contained 1.0 *w*% BHT or Ionox 220, 0.75 *w*% Uvinul 3039, or 5.0 *w*% TBAC or TOTM. A production blank (i.e. reference sample) was produced, as well.

Compoundation was performed with LTE 26-44 twin-screw extruder (Labtech Engineering Co., Ltd., Samutprakarn, Thailand) which was equipped with 26 mm diameter screws. Its rotational speed was 50 rpm during processing. The temperature profile of the screw segments was 170–175–180–185–190 °C toward the nozzle. The average output was 60 m/min of 3 mm diameter plastic filament. 3 mm long pellets were shredded using a LZ-120/VS pelletizer (Labtech Engineering Co., Ltd., Samutprakarn, Thailand).

The injection molding instrument was an Arburg Allrounder Advance 270S 400-170 (Arburg GmbH, Lossburg, Germany) with a 30 mm diameter screw. The temperature profile increased from 190 °C to 210 °C (PLA) and 170 °C to 190 °C (PP) in 5 °C steps. Molding temperature was 25 °C. Injection speed was 50 cm^3/s. Holding pressure was 500 bar for 20 s in the case of PLA and 350 bar for 5 s for PP. The residual cooling times of PLA and PP were 40 s and 20 s, respectively. The result of each injection molding cycle was a pair of 80×80×2 mm (height×width×thickness) plastic sheets.

2.3. Characterization of Plastic Materials

For the mechanical and thermal characterization of plastics, differential scanning calorimetrical (DSC) analysis and melt flow rate (*MFR*) measurement were performed. The DSC thermal analyzer (Q2000) was the product of TA Instruments (New Castle, Delaware, USA). The DSC curves were recorded in heat/cool/heat scan cycles. The purge gas was nitrogen. The mass of samples was between 3–6 mg. In the case of PLA, the examined temperature range was 0–200 °C at 5 °C/min heating and cooling rates. For PP analysis, the temperature range was –50–200 °C at 10 °C/min heating and cooling rates. The thermograms were evaluated using TA Universal Analysis Software (TA Instruments, New Castle, Delaware, USA). From the thermograms, glass transition temperature (T_g), melting temperature (T_m), enthalpy of fusion (ΔH_m), and enthalpy of cold-crystallization (ΔH_{cc}) were determined. The crystallinity ($X\%$) of plastics was calculated using the following formula:

$$X\% = \frac{\Delta H_\mathrm{m} - \Delta H_\mathrm{cc}}{\Delta H_\mathrm{f} \cdot (1-\alpha)} \cdot 100, \qquad (1)$$

where α is the amount of the additive in the plastic. The melting enthalpy of 100% crystalline (ΔH_f) PLA is 93.0 J/g **(Battegazzore et al., 2011)** and 207.1 J/g for PP **(Wunderlich, 2015)**.

MFR was measured using a CEAST 7027.000 (Instron, Norwood, Massachusetts, USA) instrument. Its operational settings were based on ISO 1133-2:2011 (ISO 1133-2:2011, 2011). The test temperature was 190 °C and the nominal load was 2.16 kg.

Both DSC and *MFR* measurements were performed in triplicate.

2.4. Migration Tests and Sample Preparation

The plastic sheets were cut into 30×10×2 mm (height×width×thickness) test specimens with a table saw. The width, length, height, and weight of each specimen were measured before immersion with Vernier callipers. The initial weights (m_{dry}) were determined using a Mettler Toledo AJ100L (Mettler Toledo, Columbus, Ohio, USA) analytical balance. The measured specimens were placed into 40 mL glass vials before adding pre-heated (40 °C) food simulants (isooctane or ethanol 95 *v*/*v*%). For the migration experiments, the surface and food simulant mass ratio recommended by Commission Regulation (EU) 10/2011 **(Commission Regulation (EU) 10/2011, 2011)** (supposing that cubic packaging with 6 dm^2 surface contains 1 kg food or food simulant) was employed, i.e. 0.6 cm^2/g food simulant. Therefore, either 18 mL isooctane or 16 mL ethanol 95 *v*/*v*% was used. Samples were stored at 40 °C in a POL-EKO ST2 laboratory incubator (Pol-Eko-Aparatura, Wodzisław Śląski, Poland). The contact times for the kinetic studies were the following: 5 min, 30 min, 1 h, 2 h, 6 h, 12 h, 1 d, 2 d, 3 d, 4 d, 5 d, 6 d, 7 d, 8 d, 9 d, 10 d, 11 d, 12 d, 13 d. For each sampling time, five parallel samples were prepared. After the defined contact times, the sample vials were removed from the incubator for immediate preparation. The weight of swelled plastic specimens (m_{swelled}) was measured after gentle wiping with a piece of blotting paper. When the concentration of a migrated compound proved to be below or above the calibration range, preconcentration or dilution was necessary (details are listed in ***Supp. Inf. Table 2***). Mirex served both as an evaporation and injection standard (ISTD). For enrichment, evaporation under a nitrogen (purity: 4.5, Messer Hungarogáz Kft., Budapest, Hungary) stream was applied. In these cases, mirex was added before the evaporation. The other samples were spiked with ISTD solution before injection into GC-EI-QMS. Eventually, every sample contained 10 mg/L mirex.

2.5. GC-EI-QMS Analysis

The quantitative analysis was performed using an Agilent 7890A gas chromatograph (Agilent Technologies, Santa Clara, California, USA) equipped with a split/splitless inlet and a 7683B autosampler coupled with an Agilent 5975C Inert XL MSD Mass Spectrometer with an electron impact ion source, quadrupole analyzer, and triple-axis detector (Agilent Technologies, Santa Clara, California, USA).

The samples were injected in split mode at a ratio of 1:10. The inlet temperature was 280 °C. The injection volume was 1 µL. A J&W DB-5MS ultra inert (Agilent Technologies, Santa Clara, California, USA) capillary column was used with dimensions of 30 m × 0.25 mm I.D. × 0.25 µm film thickness. The carrier gas was helium (purity: 5.0, Messer Hungarogáz Kft., Budapest, Hungary) with a flow rate of 2.0 mL/min. The oven temperature was 100 °C initially, then it was raised to 250 °C, at a rate of 30 °C/min. This temperature was maintained for 4.5 min, then increased to 320 °C for 2.3 min at a rate of 30 °C/min. The final temperature was maintained for 4 min. The electron impact (EI) ion source of the mass spectrometer was applied with 70 eV ionization energy. The temperature of the ion source was 230 °C and the quadrupole analyzer operated at 150 °C. The mass spectrometer was tuned with perfluorotributylamine (PFTBA, CAS: 311-89-7). For the quantitative analysis, single ion monitoring (SIM) mode was used. The qualifier and quantifier ions of target compounds are summarized in ***Table 1***. The GC-EI-QMS was controlled using Agilent MSD ChemStation (E.02.02) software.

2.6. Data Evaluation

2.6.1. Swelling degree

From the mass of the initial (m_{dry}) and swelled (m_{swelled}) plastic specimen, the swelling degree ($SD\%$) can typically be determined using the following formula:

$$SD\% = \frac{m_{\text{swelled}} - m_{\text{dry}}}{m_{\text{dry}}} \cdot 100. \qquad (2)$$

But the migration of additives causes a considerable decrease in the weight of the specimen, so it was decided that the adjusted swelling degree ($ASD\%$) should be calculated instead:

$$ASD\% = \frac{(m_{\text{swelled}} + c_{V,\text{mig,i}} \cdot V_{\text{simulant}}) - m_{\text{dry}}}{m_{\text{dry}}} \cdot 100, \qquad (3)$$

where $c_{V,\text{mig,i}}$ is the mass concentration of *i* additive (mass of migrated *i* additive normalized to the volume of food simulant) and V_{simulant} is the volume of the food simulant. To investigate the swelling kinetic, $ASD\%$ was plotted as the function of contact time.

2.6.2. Surface normalized concentration of the migrant

Based on the measured dimensions (length, width, and height), the surface area of each specimen (A_{specimen}) was calculated. The results of quantitative analysis with GC-EI-QMS give information about the mass concentration of additive *i* in the food simulant ($c_{V,\text{mig,i}}$). To consider the slight differences in the size of the test specimens, the surface normalized concentration of the migrants ($c_{A,\text{mig,i}}$) was calculated from $c_{V,\text{mig,i}}$:

$$c_{A,\text{mig,i}} = \frac{c_{V,\text{mig,i}} \cdot V_{\text{simulant}}}{A_{\text{specimen}}}. \qquad (4)$$

On the migration kinetic curves, $c_{A,\text{mig,i}}$ was plotted as the function of contact time. The extent of migration was characterized by the maximum value of $c_{A,\text{mig,i}}$ for all cases, regardless of the presence or lack of a steady-state at the end of the migration experiment.

2.6.3. Pearson's correlation test

The supposed relationship between the swelling of the plastic and the additive migration was investigated using *Pearson*'s linear correlation test. Therefore, *ASD%* was plotted as the function of $c_{A,\mathrm{mig,i}}$, and *Pearson*'s correlation coefficient (*PCC*) was calculated using OriginPro 2018 (OriginLab Corporation, Northampton, Massachusetts, USA). When the *PCC* value was above 0.9000, a strong correlation was assumed between *ASD%* and $c_{A,\mathrm{mig,i}}$.

2.6.4. Empirical semivariogram

Empirical semivariograms were calculated and plotted to assess the temporal autocorrelation structure of the concentrations of migrants and swelling degrees. **Kovács et al. (2012)** give a description of the variogram in which $Z(x)$ and $Z(x+h)$ represent two of the values measured for a particular parameter, and these two are at a distance h from each other. The distance h might be distance in time or in space. Proceeding from this, a value for the variance of the difference of $Z(x)$ and $Z(x+h)$ can be found, thus:

$$D^2[Z(x)-Z(x+h)] = D^2[Z(x)] + D^2[Z(x+h)] - 2cov[Z(x), Z(x+h)]. \tag{5}$$

Furthermore, if it is the case that the samples under consideration derive from the same population, then the following assumption may be made

$$D^2[Z(x)] = D^2[Z(x+h)], \tag{6}$$

and therefore

$$D^2[Z(x)-Z(x+h)] = 2D^2[Z(x)] - 2cov[Z(x), Z(x+h)] = 2\gamma(h) \tag{7}$$

The function expressed by $2\gamma(h)$ is the parameter's variogram, and from this, $\gamma(h)$ then represents its semivariogram. With the use of simplified notation

$$D^2[Z(x)] = D^2(x), \tag{8}$$

and

$$cov[Z(x), Z(x+h)] = g(h), \tag{9}$$

so

$$\gamma(h) = D^2(x) - g(h). \tag{10}$$

It is then possible to use the Matheron algorithm **(Matheron, 1965)** to calculate the empirical semivariogram

$$\gamma(h) = \frac{1}{2N(h)} \sum_{i=1}^{N(h)} [Z(x_i) - Z(x_i+h)]^2, \tag{11}$$

in which $N(h)$ is the number of pairs to be found within a lag interval h.

In this study, $Z(x)$ corresponds to the value of the parameter measured (e.g. $ASD\%$, $c_{A,\mathrm{mig,i}}$) in time t and h to the time interval.

Of the semivariograms thus obtained, four types can be distinguished:

a) When the semivariogram increases continuously over the distance (be it time or space) examined. In this case, the given process does not reach a steady-state.

b) When the values of the empirical semivariogram fluctuate randomly around a constant after the initial rise. In general, the value at which this occurs on the vertical axis is called a *sill*. On the horizontal axis, it is called range. Since in the present work variography is applied to kinetic curves, these range values specify the starting points (in time) of the steady-state.

c) When the empirical semivariogram on the vertical axis does not start from the origin, or the initial ascending part of the curve is missing, so the points of the semivariogram fluctuate around the variance, a nugget-effect type variogram is obtained. It should be noted that this effect may result from inadequate sampling or measurement errors **(Hatvani et al., 2012)**.

d) When the increase ends with variation around a constant, and this is repeated a number of times, i.e multiple ranges can be determined. This type of semivariogram is called a nested semivariogram. It indicates that more than one process has an influence on the variation of the data.

2.6.5. Analysis of variance (ANOVA)

The significance of differences was tested using ANOVA. The normal distribution of the data was verified using the Shapiro-Wilk test **(Shapiro & Wilk, 1965)**, the homoscedasticity assumption was assessed by Bartlett's test. Due to the absence of homoscedasticity, Welch's ANOVA was used, after which the Games-Howell *post-hoc* test was applied to compare all possible pairs of additives **(Welch, 1951)**. In the significance tests the maximum migrated concentrations were compared for each of the PP and PLA samples. The same analysis was performed with adjusted swelling degree data.

3. Results and discussion

3.1. Mechanical and thermal properties of produced plastics

The main mechanical and thermal properties of the plastics examined are summarized in ***Table 2***. *MFR* gives information about the flow properties of plastics, indirectly about their molecular weight and dynamic viscosity in a molded state. The presence of a plasticizer in

PLA moderately influences the mechanical and thermal properties. PLAs containing TBAC or TOTM have an increased *MFR* value compared to the reference plastic. Plasticizers also change the glass transition temperature (T_g) by slightly decreasing it. In the first heat cycle in the DSC analysis of PLA, the exotherm peak of cold-crystallization appears: T_{cc} of PLA reference was 95.3 ± 0.3 °C, which fell to 86.3 ± 0.3 °C and 81.0 ± 0.1 °C due to TBAC and TOTM, respectively. Some increase in the *MFR* value can be observed for BHT and Uvinul 3039 as well, but the other parameters show no distinct tendencies. Compoundation of PP with additives (besides the Irgafos 168 that it originally contained) resulted in the increase in *MFR*, irrespective of the function of additives. Otherwise, plastic additives at this level of concentration hardly influence the thermal and mechanical properties of PP.

3.2. Swelling of PLA and PP in isooctane and ethanol 95 v/v%

3.2.1. The effect of food simulant on swelling

Even though isooctane and ethanol 95 *v*/*v%* are both commonly used as solvents to substitute fatty food in migration tests, their physical-chemical characteristics differ considerably. The difference can be observed in their ability to swell PP and PLA, as well. ***Figures 1.A and 1.C*** show the swelling kinetic curves of the reference PLA (no additive) and PP (with only Irgafos 168) samples, respectively.

The swelling of PLA in isooctane was negligible. Moreover, a slight but unquestionable mass reduction was observed. Since this plastic did not contain any plastic additive, this weight reduction cannot be explained by the migration of any substance. It might be supposed that the decrease is the result of polymer degradation or solubilization. The non-swelling effect of isooctane on PLA was also reported by **Sato et al. (2012)**, however the solubility test they performed lasted only for 24 hours, and the contact temperature was only 35 °C.

Ethanol molecules are smaller than isooctane molecules and their polarity is closer to that of PLA. Consequently, PLA swelling in ethanol 95 *v*/*v%* shows a different pattern. In this case, in the thirteen days of the experiment, the swelling could not reach a lasting steady-state. As the semivariogram in ***Figure 1.B*** shows the increase of the *ASD%* came to a short halt at 112 h, but then it continued without reaching any further steady-states. The maximum value of *ASD%* (equal to *SD%* in this case) was 2.8 ± 0.03%. Comparing this result to the work of **Iñiguez-Franco et al. (2012)**, the notable effect of test specimen thickness on swelling can be seen: they found that neat PLA film (with 27.9 ± 9.9 μm thickness) reached swelling equilibrium almost immediately with 6% ethanol sorption.

PP swells in both food simulants, however; due to its non-polar character, the absorption of isooctane is more than one order of magnitude higher than that of ethanol. In isooctane, the *ASD%* increases up to 165 h (based on its empirical semivariogram), at which point a long-lasting steady-state starts at 8.9 ± 0.15%. On the other hand, the swelling of PP in ethanol 95 *v*/*v%* shows an unconventional pattern (***Figure 1.D***). After the initial increase of *ASD%* a steady-state starts to form at 68 h, but instead of stabilizing permanently, the *ASD%* starts to increase again to reach a second plateau at 0.24 ± 0.01%, starting at 210 h. This results in a nested semivariogram, and this behaviour suggests that the swelling advances layer by layer, in accordance with the fact that polymer chain orientation varies along the cross-section of test specimens. This heterogeneity in chain orientation is the result of fountain flow in the injection molding process.

3.2.2. The effect of plastic additive's function on swelling

The kinetic curves of the swelling of the various PLA samples in ethanol 95 *v*/*v%* and that of PP samples in isooctane – i.e. the solvent having a stronger swelling effect – are presented in ***Figures 2.A*** and ***2.B***. As expected, they show that plasticizers (TBAC and TOTM) promote the swelling of both polymers. The maximum values of *ASD%* in the case of PLA with no additive (reference), PLA–BHT, PLA–Ionox 220, and PLA–Uvinul 3039 are between 2.8 ± 0.03% and 3.1 ± 0.03% in ethanol 95 *v*/*v%*. The statistical analysis proved that there is no significant difference (α=0.05) in the swelling of neat and antioxidant or UV stabilizer spiked PLA, even though the *MFR* values of the PLA–BHT and PLA–Uvinul 3039 plastics are moderately elevated compared to the reference PLA. Meanwhile, the maximum *ASD%* of PLA–TBAC and PLA–TOTM are 6.4 ± 0.10% and 4.3 ± 0.23%, respectively. This increase in the *ASD%* values of the two plasticizer-spiked PLAs is a result of the polymer chain mobilizing effect of these additives.

The *ASD%* values for PP in isooctane at the end of the experiment for the plastics with various additives fall within a narrow range (8.8 ± 0.08%–10.7 ± 0.10)%. However, the statistical analysis revealed significant difference between PP with stabilizers and PP with plasticizers. The plasticizing effect which facilitates easier swelling is even more apparent in the slopes of the kinetic curves in the first 4 days of the experiments. Due to the faster swelling, PP–TBAC and PP–TOTM reaches the steady-state at 44 h and 60 h, respectively. Whereas, the samples without plasticizer took about 113–167 h to reach the final degree of swelling. These results imply that the *ASD%* of PLA samples may eventually rise to a similar value, too. But 13 days' contact time was clearly not enough to reach the equilibrium of the PLA–ethanol system.

3.3 Migration of additives

3.3.1. Migration in different polymer-solvent systems

The surface normalized concentrations of the migrated additives as a function of time provided different patterns for each of the polymer–food simulant pairs. In all cases, significant differences ($\alpha=0.05$) were found using Welch's ANOVA among the maximum of migrated concentrations (see ***Table 3***). Furthermore, the significant difference for all possible pairs was confirmed using the post-hoc test. As an example, both the swelling and migration kinetic curves of the polymers containing TBAC are presented in ***Figure 3***, whereas ***Table 3*** lists the maximum observed concentrations of every additive. Isooctane does not swell PLA, consequently, the additives appearing in the solvent within the 13 days come from the surface layer of the plastic. Thus, the concentrations in the isooctane phase remain so low that their measurement could be carried out only with a relatively high degree of uncertainty. Furthermore, the mass transfer from the surface is prompt. As a result of these two factors, nugget-effect type semivariograms were obtained for all additives in the PLA–isooctane system.

In the PLA–ethanol systems for all additives, the maximum of the surface normalized concentrations was three orders of magnitude higher. Within the 13 days of the experiments, equilibrium could not be reached for any of the additives. Both the swelling and the migration curves show an indisputably increasing trend, even though the rate of the increase is not constant: at least one short halt can be detected in all cases.

For PP, the situation is reversed. Ethanol can only slightly penetrate PP, but isooctane swells it considerably. Consequently, migration of the additives studied from PP into isooctane gave typically concentrations in the solvent phase one order of magnitude higher than that into ethanol 95 *v*/*v*%. With the exception of BHT, the migration curves in the PP–isooctane systems showed a dynamically increasing initial part, which between 63 h and 255 h turned into a presumably long-lasting steady-state. But the migration of BHT into isooctane slowed down for a short while and then increased again to reach a lasting steady-state at 163 h. Such changes in the rate of increase of the migrated concentrations were, however, much more characteristic of the PP–ethanol systems. These halts and plateaus in the increase of surface normalized concentrations in the liquid phase of the PLA–ethanol and the PP–

ethanol systems indicate that not only the swelling, but also the migration proceeds layer by layer. The observation of this phenomenon was facilitated by the use of unusually thick test specimens.

The effect of swelling on the migrant concentrations can be observed clearly on the maximum values of surface normalized concentrations as well. For all additives, the highest concentrations were observed when PP was in contact with isooctane, that is, where the swelling was the most intense. A similar observation was made by **Alin & Hakkarainen (2010)**, who investigated the migration of two antioxidants (Irganox 1010 and Irgafos 168) from PP-based FCP into various food simulants by microwave irradiation. In their research they found that the amount of Irganox 1010 and Irgafos 168 was approximately 40 and 20 times higher in isooctane than in ethanol 95 *v*/*v*%, respectively **(Alin & Hakkarainen, 2010)**.

Isooctane with PLA provided the lowest concentrations, in agreement with the lack of swelling. Ethanol was absorbed by both PLA and PP, but not to the same extent. The *ASD%* values for PLA samples were about one order of magnitude higher than those for the PP samples. Accordingly, for every additive, the concentrations in ethanol 95 *v*/*v%* were higher when they migrated from the PLA.

3.3.2. Molecular weight of additives and migration

For the comparison of the observed concentrations in the food simulants across the different additives, one must take into consideration the fact that for the preparation of the plastics, the additives were applied in different mass ratios. ***Figure 4*** shows the surface normalized concentrations divided by the applied mass ratios for both PLA and PP.

For the stabilizer additives (BHT, Ionox 220, Uvinul 3039, and Irgafos 168), a clear tendency can be observed in the migration concentrations: as the molecular weights of the additives increase, the migrated concentrations decrease. The diffusion of chemical compounds is an essential part of migration from plastics which thus depends directly on the hydrodynamic or Stokes radius of the migrating molecule at a given temperature and hence, indirectly, on its molecular weight. Beyond molecular weight, the size and shape of the migrating compound, and its affinity to the formation of intermolecular interactions can be essential in the process of migration. **Samsudin et al. (2014)** in their work compared their results (for astaxanthin release) with previous antioxidant migration studies from PLA. They noticed that the diffusion coefficient of BHT (**Ortiz-Vazquez et al., 2011**) is at least twice as high as any other antioxidant's. The presumed explanation for the higher migration rate was the BHT molecule's non-bulky structure, compared to the other compounds examined. **Samsudin et al.**

(2014) also considered the theory of **Iñiguez-Franco et al. (2012)** concerning the number of hydroxyl groups in the migrating compound molecule, which speculates that the presence of this functional group decreases the release rate.

The pattern expected on the basis of the additives' molecular weight is disturbed by the plasticizers. According to the molecular weight of the additives, the expected order of maximum migration concentration would be: Irgafos 168 (PP only) < TOTM < Ionox 220 < TBAC < Uvinul 3039 < BHT. However, in PLA the order was: Ionox 220 < TOTM < Uvinul 3039 < BHT < TBAC; while in PP it was: Irgafos 168 < Ionox 220 < Uvinul 3039 < BHT < TOTM < TBAC. The reason of the change is the chain mobilizing effect of the plasticizers.

TBAC facilitated its own diffusion among the polymer chains of both PLA and PP to such an extent that its migration concentrations went higher than that of all the smaller stabilizer additives (BHT, Ionox 220 and Uvinul 3039). In the PP–isooctane system, the same happens for TOTM, hence its curve on ***Figure 4*** closely approaches that of TBAC instead of Irgafos 168. But the plasticizing effect of TOTM in PLA was not as intense as that of TBAC. As ***Figure 2.A*** shows, the swelling of PLA–TOTM is approximately in the middle between the PLA–TBAC and the other PLA-based plastics. This is in accordance with the picture in ***Figure 4***, in which its curve moves just a bit above that of Ionox 220 even though its higher molecular weight would suggest otherwise. On the other hand, the plasticizing effect of TOTM was enough for a moderate enhancement of the swelling, which in turn was able to facilitate its migration somewhat over the migration of the next additive in line. But this effect was not strong enough to elevate this migration to the level of the smaller additives, let alone TBAC.

3.4. Correlation between swelling degree and migrated concentration of additives

Both swelling and migration kinetic curves displayed various shapes. As detailed in the previous sections, there were occasions when the change in the relevant parameter was small compared to the degree of uncertainty in its measurement. In the case of the most intense swellings and migrations, the curves reached a steady-state after a consistent increase at the beginning of the experiments. A stepwise increase was also often observed. Even amid this great variety, the corresponding swelling and migration curves always followed the same pattern. To demonstrate that the similarity in the shapes of the curves is a result of a strong relationship between the two processes, *ASD%* and $c_{A,\mathrm{mig,i}}$ values were correlated. Since the isooctane absorption of PLA was negligible, these cases were not considered. For all the other polymer–additive–solvent systems the obtained *Pearson's* correlation coefficients showed a strong linear correlation, as they ranged between 0.9664 and 0.9924, except for Uvinul 3039 in PP–isooctane, for which the value was 0.9134.

Figure 5 demonstrates the relation between the swelling and migration curves of the PLA–Uvinul 3039 (***Figure 5.A***) and the PP–BHT (***Figure 5.B***) samples in contact with ethanol 95 *v*/*v*%. Their respective semivariograms are also shown. Both of these curves show stepwise processes. In the case of PLA–Uvinul 3039, neither the swelling nor the migration could reach steady-state. Still, short halts in the increase of the respective parameter can be observed. The presence of these is confirmed for both curves by their nested semivariograms. Moreover, with the help of the variograms, the starting points of these halts can be identified. As ***Figure 5.A*** shows, in this case starting points on the two curves follow each other closely, there is no significant difference between the time pairs.

Figure 5.B also shows a stepwise increase for both swelling and migration for the PP–BHT samples. In this case, however, the starting points in the migration curve are considerably delayed with respect to those in the swelling curve. As a result, only two starting points can be detected in the migration curve within the 13 day timeframe of the experiment, whereas the swelling curve has three. It is safe to assume that over the 13 days, a further increase in the concentration of BHT in the ethanol 95 *v*/*v*% could be observed.

The starting points identified by the semivariograms for the other polymer–additive pairs are listed in ***Table 4***. Most of the data follow one or other of the above-described patterns: practically equal starting points or considerably delayed migration. In some cases (e.g. PP–Uvinul 3039 in ethanol 95 *v*/*v*%), the delay at the first detected point is negligible, but by the second plateau, the delay becomes obvious. Either way, the migration always follows the swelling, even if closely. The only exception seems to be Ionox 220 migrating from PLA to ethanol 95 *v*/*v*%. In this case, the first halt in the migration is so short that the corresponding halt in the swelling curve could only be detected after increasing the frequency of the sampling. Unfortunately, the presence and the extent of the delays shows no apparent pattern. Consequently, the time necessary to reach a steady-state on the migration curve cannot be predicted on the basis of the swelling curve.

4. Conclusions

In the present work, the time dependence of the migration of commonly used plastic additives from polylactic acid (PLA) and polypropylene (PP) to ethanol 95 *v*/*v*% and isooctane was investigated in 13 day long experiments. Alongside the measurement of the concentration of the additives in these food simulants, the swelling of the test specimens was followed. As expected, a strong correlation was observed between the two processes.

PLA cannot be swelled by isooctane, but it is penetrated by ethanol, whereas PP is swelled to a great degree by isooctane and only slightly by ethanol. For all polymer-food simulant pairs, where swelling can be observed, the addition of plasticizers increased the rate and degree of swelling, though this change had a smaller effect than changing the polymer or the food simulant in the experimental setting.

Both for swelling and migration, a stepwise increase in the relevant parameter was observed. Short halts in the increase were characteristic rather of the PLA–ethanol systems, whereas clear plateaus formed when PP was in contact with ethanol 95 *v*/*v*%. The kinetic curves of the PP samples in isooctane were, in general, more regular: they consisted of a dynamically increasing initial part, which turned into a lasting steady-state.

Regardless of the shape of the kinetic curves, for all additives the greater the swelling, the higher migration concentrations observed. This relation between swelling and migration has an important implication. Whenever isooctane and ethanol 95 *v*/*v*% as simulants are used for fatty food instead of vegetable oil, the decision on the compliance of the tested plastic must be based on the highest observed migration concentrations to ensure food safety. If the migration tests are performed only in the solvent that provides these higher concentrations, the number of experiments can be about half of what would otherwise be allotted. The results presented here suggest that for additives that are well soluble in both simulants, the solvent that can better penetrate the plastic should be used. On the other hand, using a solvent that swells the polymer much better than vegetable oil will probably result in the extreme overestimation of the migration.

The diffusion of the additives is an essential part of their migration to food simulants. So, the hydrodynamic or Stokes radius of the migrating molecule and thus, indirectly, the molecular weight may be expected to influence the concentration of the migrants. Accordingly, the migration of stabilizers from PLA to ethanol 95 *v*/*v*%, as well as from PP to isooctane decreased with increasing molecular weight. But the migration of TBAC was stronger in both cases, even though its molecular weight is bigger than that of BHT and

Uvinul 3039. This means that the promoting effect of plasticizing on swelling and thus migration outweighed the demoting effect of the higher molecular mass.

The strong correlation between the swelling degree and migration concentrations was confirmed by the fact that the values of *Pearson's* correlation coefficients were over 0.9100. Furthermore, variography was successfully employed in the determination of the start of plateaus on the kinetic curves. In the case of PLA–isooctane systems, nugget-effect type empirical semivariograms were obtained due to the low level of migration and the comparatively high uncertainty of the concentration results. But for all other cases, the semivariograms could objectively highlight the starting points of both short halts and somewhat longer plateaus in the increase of either the swelling degree or the migrant concentration. The result thus obtained unambiguously showed that migration, either closely or loosely, nonetheless strictly follows the swelling even in the case of multiple-level curves.

All these results prove that the extent of the migration of a certain additive should not be estimated solely on parameters characterizing the materials alone (additive, polymer and food simulant). Rather, it is the interactions between these parameters, especially the plasticizing effect of either the additive or the solvent, that are fundamental.

Acknowledgement

We are thankful to Wessling International Research and Education Center (WIREC) for providing financial support, laboratory equipment, and materials for our research. The authors gratefully acknowledge the helpful work of the technical staff of Budapest University of Technology and Economics, Faculty of Mechanical Engineering, Department of Polymer Engineering in the manufacture of plastic specimens. We are also thankful to BASF Hungary Ltd. for donating Uvinul 3039.

This research program has been implemented with support provided by the National Research, Development and Innovation Fund of Hungary, financed under project No. 128440 of the FK18 funding scheme and from the Hungarian Ministry of Human Capacities financed under the ELTE Institutional Excellence Program (TKP2020-IKA-05). This work was supported by the National Research, Development, and Innovation Office, Hungary (2019-1.1.1-PIACI-KFI-2019-00205, 2017-2.3.7-TÉT-IN-2017-00049, OTKA FK134336). The research reported in this paper and carried out at BME is supported by the NRDI Fund (TKP2020 NC, Grant No. BME-NCS) based on the charter of bolster issued by the NRDI Office under the auspices of the Ministry for Innovation and Technology. This paper was supported by the János Bolyai Research Scholarship of the Hungarian Academy of Sciences. The research was supported by the ÚNKP-20-5 New National Excellence Program of the Ministry for Innovation and Technology from the source of the National Research, Development and Innovation Fund. This publication was supported by the Italian-Hungarian bilateral agreement (grant number NKM 73/2019) of the Hungarian Academy of Sciences.

CRediT (Contributor Roles Taxonomy) authorship contribution statement

Csaba Kirchkeszner: conceptualization, design and conduct the experiments, data evaluation and visualization, formal analysis, writing – original draft

Noémi Petrovics: conceptualization, design and conduct the experiments, data evaluation and visualization, formal analysis, writing – original draft

Tamás Tábi: production and analysis of plastics, data interpretation, writing – review & editing, funding acquisition

Norbert Magyar: data visualization, formal analysis, writing – review & editing

József Kovács: data visualization, formal analysis, writing – review & editing, funding acquisition

Bálint Sámuel Szabó: writing – review & editing, conceptualization

Zoltán Nyiri: writing – review & editing, conceptualization

Zsuzsanna Eke: conceptualization, supervision, writing – review & editing, funding acquisition

References

Alin, J., & Hakkarainen, M. (2010). Type of polypropylene material significantly influences the migration of antioxidants from polymer packaging to food simulants during microwave heating. *Journal of Applied Polymer Science*, *118*(2), 1084–1093. https://doi.org/10.1002/app.32472

Aznar, M., Ubeda, S., Dreolin, N., & Nerín, C. (2019). Determination of non-volatile components of a biodegradable food packaging material based on polyester and polylactic acid (PLA) and its migration to food simulants. *Journal of Chromatography A*, *1583*, 1–8. https://doi.org/10.1016/j.chroma.2018.10.055

Battegazzore, D., Bocchini, S., & Frache, A. (2011). Crystallization kinetics of poly(lactic acid)-talc composites. *Express Polymer Letters*, *5*(10), 849–858. https://doi.org/10.3144/expresspolymlett.2011.84

Bodai, Z., Kirchkeszner, C., Novák, M., Nyiri, Z., Kovács, J., Magyar, N., Iván, B., Rikker, T., & Eke, Z. (2015). Migration of Tinuvin P and Irganox 3114 into milk and the corresponding authorised food simulant. *Food Additives and Contaminants - Part A Chemistry, Analysis, Control, Exposure and Risk Assessment*, *32*(8), 1358–1366. https://doi.org/10.1080/19440049.2015.1055523

Chang, Y., Kang, K., Park, S. J., Choi, J. C., Kim, M. K., & Han, J. (2019). Experimental and theoretical study of polypropylene: Antioxidant migration with different food simulants and temperatures. *Journal of Food Engineering*, *244*(February 2018), 142–149. https://doi.org/10.1016/j.jfoodeng.2018.09.028

European Commission (2011). Plastic materials and articles intended to come into contact with food. *European Commission Regulation No 10/2011 EC.* Available at: https://eur-lex.europa.eu/legal-content/EN/TXT/?uri=CELEX%3A02011R0010-20200923

Feigenbaum, A. E., Riquet, A. M., & Scholler, D. (2000). Fatty food simulants: Solvents to mimic the behavior of fats in contact with packaging plastics. In *ACS Symposium Series* (Vol. 753, Issue 1, pp. 71–81). https://doi.org/10.1021/bk-2000-0753.ch007

Garde, J. A., Catalá, R., Gavara, R., & Hernandez, R. J. (2001). Characterizing the migration of antioxidants from polypropylene into fatty food simulants. *Food Additives and Contaminants*, *18*(8), 750–762. https://doi.org/10.1080/02652030116713

Gavriil, G., Kanavouras, A., & Coutelieris, F. A. (2018). Food-packaging migration models: A critical discussion. *Critical Reviews in Food Science and Nutrition*, *58*(13), 2262–2272. https://doi.org/10.1080/10408398.2017.1317630

Hatvani, I., Kovács, J., & Korponai, J. (2012). Mintavételezési gyakoriság optimalizálása variogram függvénnyel a Kis-Balaton Vízvédelmi Rendszer példáján. *Természetvédelmi Közlemények*, *18*(Pomogyi 1991), 202–210.

Hatvani, G., Kirschner, A. K. T., Farnleitner, A. H., Tanos, P., & Herzig, A. (2018). Hotspots and main drivers of fecal pollution in Neusiedler See, a large shallow lake in Central Europe. *Environmental Science and Pollution Research*, *25*(29), 28884–28898. https://doi.org/10.1007/s11356-018-2783-7

Hatvani, G., Erdélyi, D., Vreča, P., & Kern, Z. (2020). Analysis of the spatial distribution of stable oxygen and hydrogen isotopes in precipitation across the Iberian Peninsula. *Water (Switzerland)*, *12*(2). https://doi.org/10.3390/w12020481

Hatvani, G., Leuenberger, M., Kohán, B., & Kern, Z. (2017). Geostatistical analysis and isoscape of ice core derived water stable isotope records in an Antarctic macro region. *Polar Science*, *13*, 23–32. https://doi.org/10.1016/j.polar.2017.04.001

Hatvani, G., Magyar, N., Zessner, M., Kovács, J., & Blaschke, A. P. (2014). Die Europäische Wasserrahmenrichtlinie: Kann man aus den Grundwassermessdaten mehr Informationen gewinnen? Eine Fallstudie im Seewinkel, Burgenland, Österreich. *Hydrogeology Journal*, *22*(4), 779–794. https://doi.org/10.1007/s10040-013-1093-x

Iñiguez-Franco, F., Auras, R., Burgess, G., Holmes, D., Fang, X., Rubino, M., & Soto-Valdez, H. (2016). Concurrent solvent induced crystallization and hydrolytic degradation of PLA by water-ethanol solutions. *Polymer*, *99*, 315–323. https://doi.org/10.1016/j.polymer.2016.07.018

Iñiguez-Franco, F., Auras, R., Rubino, M., Dolan, K., Soto-Valdez, H., & Selke, S. (2017). Effect of nanoparticles on the hydrolytic degradation of PLA-nanocomposites by water-ethanol solutions. *Polymer Degradation and Stability*, *146*, 287–297. https://doi.org/10.1016/j.polymdegradstab.2017.11.004

Iñiguez-Franco, F., Soto-Valdez, H., Peralta, E., Ayala-Zavala, J. F., Auras, R., & Gámez-Meza, N. (2012). Antioxidant activity and diffusion of catechin and epicatechin from antioxidant active films made of poly(l-lactic acid). *Journal of Agricultural and Food Chemistry*, *60*(26), 6515–6523. https://doi.org/10.1021/jf300668u

ISO 1133-2:2011 (2011). *Plastics – Determination of the melt mass-flow rate (MFR) and melt volume-flow rate (MVR) of thermoplastics – Part 2: Method for materials sensitive to time-temperature history and/or moisture.* International Organization for Standardization.

Jamshidian, M., Tehrany, E. A., & Desobry, S. (2012). Release of synthetic phenolic antioxidants from extruded poly lactic acid (PLA) film. *Food Control*, *28*(2), 445–455. https://doi.org/10.1016/j.foodcont.2012.05.005

Jamshidian, M., Tehrany, E. A., & Desobry, S. (2013). Antioxidants Release from Solvent-Cast PLA Film: Investigation of PLA Antioxidant-Active Packaging. *Food and Bioprocess Technology*, *6*(6), 1450–1463. https://doi.org/10.1007/s11947-012-0830-9

Kang, K., Chang, Y., Choi, J. C., Park, S. J., & Han, J. (2018). Migration Study of Butylated Hydroxytoluene and Irganox 1010 from Polypropylene Treated with Severe Processing Conditions. *Journal of Food Science*, *83*(4), 1005–1010. https://doi.org/10.1111/1750-3841.14104

Kern, Z., Erdelyi, D., Vreča, P., Krajcar Bronić, I., Forizs, I., Kandu, T., Štrok, M., Palcsu, L., Suveges, M., Czuppon, G., Kohan, B., & Hatvani, I. G. (2020). Isoscape of amount-weighted annual mean precipitation tritium (3H) activity from 1976 to 2017 for the Adriatic-Pannonian region - AP3H_v1 database. *Earth System Science Data*, *12*(3), 2061–2073. https://doi.org/10.5194/essd-12-2061-2020

Kovács, J., Korponai, J., Székely Kovács, I., & Hatvani, I. G. (2012). Introducing sampling frequency estimation using variograms in water research with the example of nutrient loads in the Kis-Balaton Water Protection System (W Hungary). *Ecological Engineering*, *42*, 237–243. https://doi.org/10.1016/j.ecoleng.2012.02.004

Kuorwel, K. K., Cran, M. J., Sonneveld, K., Miltz, J., & Bigger, S. W. (2013). Migration of antimicrobial agents from starch-based films into a food simulant. *LWT - Food Science and Technology*, *50*(2), 432–438. https://doi.org/10.1016/j.lwt.2012.08.023

Lu, W., Jiang, K., Chu, Z., Yuan, M., Tang, Z., & Qin, Y. Y. (2021). Changes of thermal properties and microstructure of nano-ZnO/polylactic acid composite films during Zn migration. *Packaging Technology and Science*, *34*(1), 3–10. https://doi.org/10.1002/pts.2535

Manzanarez-López, F., Soto-Valdez, H., Auras, R., & Peralta, E. (2011). Release of α-Tocopherol from Poly(lactic acid) films, and its effect on the oxidative stability of soybean oil. *Journal of Food Engineering*, *104*(4), 508–517. https://doi.org/10.1016/j.jfoodeng.2010.12.029

Mascheroni, E., Guillard, V., Nalin, F., Mora, L., & Piergiovanni, L. (2010). Diffusivity of propolis compounds in Polylactic acid polymer for the development of anti-microbial packaging films. *Journal of Food Engineering*, *98*(3), 294–301. https://doi.org/10.1016/j.jfoodeng.2009.12.028

Matheron, G. (1965). *JOURNAL DE LA SOCIÉTÉ STATISTIQUE DE PARIS Présentation des variables régionalisées*. *107*, 263–275.

Nasiri, A., Peyron, S., Gastaldi, E., & Gontard, N. (2016). Effect of nanoclay on the transfer properties of immanent additives in food packages. *Journal of Materials Science*, *51*(21), 9732–9748. https://doi.org/10.1007/s10853-016-0208-x

Ortiz-Vazquez, H., Shin, J., Soto-Valdez, H., Auras, R. (2011). Release of butylated hydroxytoluene (BHT) from Poly(lactic acid) films. *Polymer Testing*, *30*(5), 463–471. https://doi.org/10.1016/j.polymertesting.2011.03.006

Ramos, M., Beltrán, A., Peltzer, M., Valente, A. J. M., & Garrigós, M. del C. (2014). Release and antioxidant activity of carvacrol and thymol from polypropylene active packaging films. *LWT - Food Science and Technology*, *58*(2), 470–477. https://doi.org/10.1016/j.lwt.2014.04.019

Samsudin, H., Auras, R., Mishra, D., Dolan, K., Burgess, G., Rubino, M., Selke, S., & Soto-Valdez, H. (2018). Migration of antioxidants from polylactic acid films: A parameter estimation approach and an overview of the current mass transfer models. *Food Research International*, *103*(July 2017), 515–528. https://doi.org/10.1016/j.foodres.2017.09.021

Samsudin, H., Soto-Valdez, H., & Auras, R. (2014). Poly(lactic acid) film incorporated with marigold flower extract (Tagetes erecta) intended for fatty-food application. *Food Control*, *46*, 55–66. https://doi.org/10.1016/j.foodcont.2014.04.045

Sato, S., Gondo, D., Wanda, T., Kanehashi, S., Nagai, K. (2012). Effects of various liquid organic solvents on solvent-induced crystallization of amorphous poly(lactic acid) film. *Journal of Applied Polymer Science*, *129*(3), 1607–1617. https://doi.org/10.1002/app.38833

Shapiro, S. S., & Wilk, M. B. (1965). *An Analysis of Variance Test for Normality (Complete Samples)* (Vol. 52, Issue 3). https://www.jstor.org/stable/2333709

Trásy, B., Garamhegyi, T., Laczkó-Dobos, P., Kovács, J., & Hatvani, I. G. (2018). Geostatistical screening of flood events in the groundwater levels of the diverted inner delta of the Danube River: Implications for river bed clogging. *Open Geosciences*, *10*(1), 64–78. https://doi.org/10.1515/geo-2018-0006

Vera, P., Canellas, E., & Nerín, C. (2018). Identification of non volatile migrant compounds and NIAS in polypropylene films used as food packaging characterized by UPLC-MS/QTOF. *Talanta*, *188*, 750–762. https://doi.org/10.1016/j.talanta.2018.06.022

Welch, B. L. (1951). *On the Comparison of Several Mean Values: An Alternative Approach* (Vol. 38, Issue 3).

Wunderlich, B. (2005). Structure and Properties of Materials. In B. Wunderlich (Ed.), *Thermal Analysis of Polymeric Materials*, (pp. 512–516). Springer.

Yang, W., Fortunati, E., Dominici, F., Giovanale, G., Mazzaglia, A., Balestra, G. M., Kenny, J. M., & Puglia, D. (2016). Effect of cellulose and lignin on disintegration, antimicrobial and antioxidant properties of PLA active films. *International Journal of Biological Macromolecules*, *89*, 360–368. https://doi.org/10.1016/j.ijbiomac.2016.04.068

Figure captions

Figure 1 Swelling kinetic curves of reference PLA (***1.A***) and PP (***1.C***) in isooctane and ethanol 95 *v*/*v*%, and their empirical semivariograms in ethanol 95 *v*/*v*% (***1.B*** for PLA and ***1.D*** for PP)

Figure 2 Swelling kinetic curves of PLA (***2.A***) in ethanol 95 *v*/*v*% and PP (***2.B***) in isooctane

Figure 3 Migration and swelling of TBAC-compounded PLA (***3.A*** and ***3.B***) and PP (***3.C*** and ***3.D***) in isooctane and ethanol 95 *v*/*v*%, respectively

Figure 4 Surface normalized concentrations divided by the applied mass ratios of the additives for PLA and PP in ethanol 95 *v*/*v*% and isooctane, respectively (Molecular weight values: M_{BHT} = 220.3 g/mol, $M_{\mathrm{Uvinul\ 3039}}$ = 361.5 g/mol, M_{TBAC} = 402.5 g/mol, $M_{\mathrm{Ionox\ 220}}$ = 424.7 g/mol, M_{TOTM} = 546.8 g/mol, $M_{\mathrm{Irgafos\ 168}}$ = 646.9 g/mol)

Figure 5 Relation between swelling and surface normalized concentrations in ethanol 95 *v*/*v*% for Uvinul 3039 from PLA (***5.A***) and BHT from PP (***5.B***)

Table captions

Table 1 Retention time, qualifier and quantifier ions, *LLOQ* and recovery (at *LLOQ*) of target compounds

Table 2 Mechanical and thermal properties of the investigated plastic samples

Table 3 Maximum surface normalized concentrations

Table 4 Starting points of steady-states in the swelling and migration curves

Table 1 Retention time, qualifier and quantifier ions, *LLOQ* and recovery (at *LLOQ*) of target compounds

Target Compounds	***Retention time*** *(min)*	***Quantifier ion*** *(m/z)*	***Qualifier ions*** *(m/z)*		***LLOQ**** (mg/L)		***Recovery at LLOQ*** (%)	
					Ethanol 95 v/v%	***Isooctane***	***Ethanol 95 v/v%***	***Isooctane***
BHT	6.67	205	145	220	0.025	0.05	104.8	112.6
Ionox 220	12.62	409	367	424	0.5	0.5	97.3	119.6
Irgafos 168	16.81	441	147	308	0.5	0.1	101.6	112.9
Uvinul 3039	12.86	249	204	360	0.5	0.5	87.3	89.1
TBAC	9.48	185	259	129	0.1	0.1	119.9	81.6
TOTM	16.97	305	193	435	0.5	0.1	89.7	108.0
Mirex (ISTD)	12.33	272	237	332	–	–	–	–

LLOQ: lower limit of quantitation

Table 4 Starting points of steady-states in the swelling and migration curves

	Additives	*Starting points of steady-states (h)*	
		Swelling	***Migration***
PLA–ethanol	**BHT**	87; 165	87; 165
	Ionox 220	111; 191	70; 143; 193
	Uvinul 3039	63; 135; 261	68; 135; 260
	TBAC	112; 167	117; 237
	TOTM	73; 112; 162	93; 147; 212
PP–ethanol	**BHT**	87; 163; 260	115; 260
	Ionox 220	60; 167	163; 260
	Irgafos 168	68; 210	116; 238
	Uvinul 3039	93; 167	117; 233
	TBAC	67; 133; 207	73; 133; 207
	TOTM	117; 213	188
PP–isooctane	**BHT**	60; 113	87; 165
	Ionox 220	114	255
	Irgafos 168	165	208
	Uvinul 3039	167	167
	TBAC	44	63
	TOTM	60	115

Table 2 Mechanical and thermal properties of the investigated plastic samples

	Additives	***MFR*** (g/10 min)	T_g (°C)	T_m (°C)	ΔH_m (J/g)	T_{cc} (°C)	ΔH_{cc} (J/g)	***X*** (%)
2500HP PLA	Reference	3.2 ± 0.1	61.1 ± 0.1	175.8 ± 0.1	46.8 ± 1.0	95.3 ± 0.3	28.1 ± 1.1	20.1 ± 0.8
	BHT	5.1 ± 0.1	61.7 ± 0.1	175.6 ± 0.1	45.4 ± 0.7	90.7 ± 0.2	24.7 ± 0.6	22.5 ± 0.8
	Ionox 220	3.4 ± 0.1	61.2 ± 0.2	175.5 ± 0.0	46.4 ± 0.4	91.4 ± 0.2	24.7 ± 1.1	23.6 ± 1.4
	Uvinul 3039	5.4 ± 0.1	61.3 ± 0.2	175.3 ± 0.2	46.1 ± 1.0	90.9 ± 0.1	26.5 ± 0.8	21.2 ± 0.4
	TBAC	6.8 ± 0.2	55.8 ± 0.2	174.4 ± 0.0	41.2 ± 1.0	86.3 ± 0.3	21.3 ± 0.9	22.5 ± 2.2
	TOTM	6.5 ± 0.1	56.3 ± 0.1	174.4 ± 0.1	46.9 ± 1.6	81.0 ± 0.1	21.4 ± 0.3	28.9 ± 2.2
H145F PP	Reference*	9.8 ± 0.1	–	165.1 ± 0.1	81.5 ± 1.0	–	–	39.4 ± 0.5
	BHT	13.9 ± 0.1	–	164.5 ± 0.2	77.6 ± 1.4	–	–	37.5 ± 0.7
	Ionox 220	13.3 ± 0.1	–	164.6 ± 0.0	87.2 ± 1.9	–	–	42.1 ± 0.9
	Uvinul 3039	14.0 ± 0.1	–	164.8 ± 0.1	81.2 ± 0.7	–	–	39.2 ± 0.3
	TBAC	15.1 ± 0.1	–	163.6 ± 0.1	82.3 ± 1.0	–	–	39.8 ± 0.5
	TOTM	14.9 ± 0.2	–	164.1 ± 0.2	80.9 ± 2.6	–	–	39.0 ± 1.2

*It contained Irgafos 168 antioxidant.

**All values are given as mean ± standard deviation.

Table 3 Maximum surface normalized concentrations

	Additives	***Maximum value of $c_{A,\mathrm{mig},i}$*** (mg/dm^2)	
		Isooctane	***Ethanol 95 v/v%***
PLA	**BHT**	0.0036 ± 0.0011	14.2 ± 1.06
	Ionox 220	0.0040 ± 0.0015	6.75 ± 0.972
	Uvinul 3039	0.0055 ± 0.00036	7.32 ± 0.514
	TBAC	0.11 ± 0.019	174 ± 15.3
	TOTM	0.043 ± 0.0082	34.1 ± 4.54
PP	**BHT**	48.2 ± 1.82	2.77 ± 0.138
	Ionox 220	31.1 ± 1.33	0.48 ± 0.040
	Irgafos 168	5.24 ± 0.150	0.032 ± 0.0010
	Uvinul 3039	32.2 ± 1.56	1.75 ± 0.067
	TBAC	339 ± 3.26	33.5 ± 0.581
	TOTM	327 ± 3.10	20.4 ± 0.776

*All values are given as mean ± standard deviation.

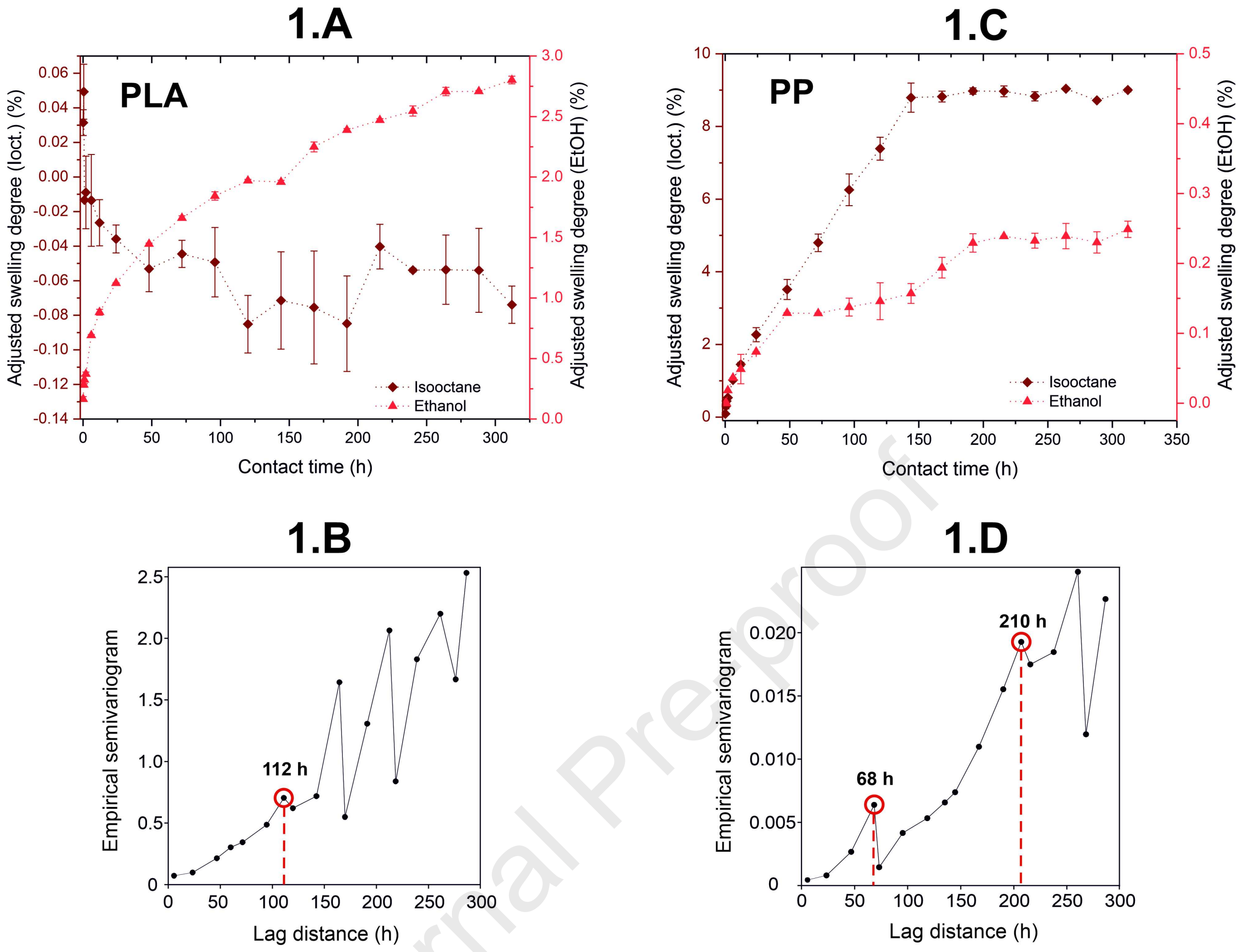
1.A
PLA
Adjusted swelling degree (Ioct.) (%)
Adjusted swelling degree (EtOH) (%)
Contact time (h)
Isooctane
Ethanol
0.06
0.04
0.02
0.00
-0.02
-0.04
-0.06
-0.08
-0.10
-0.12
-0.14
3.0
2.5
2.0
1.5
1.0
0.5
0.0
0
50
100
150
200
250
300
1.C
PP
Adjusted swelling degree (Ioct.) (%)
Adjusted swelling degree (EtOH) (%)
Contact time (h)
Isooctane
Ethanol
10
8
6
4
2
0
0.5
0.4
0.3
0.2
0.1
0.0
0
50
100
150
200
250
300
350
1.B
Empirical semivariogram
Lag distance (h)
112 h
2.5
2.0
1.5
1.0
0.5
0
0
50
100
150
200
250
300
1.D
Empirical semivariogram
Lag distance (h)
68 h
210 h
0.020
0.015
0.010
0.005
0
0
50
100
150
200
250
300

2.A

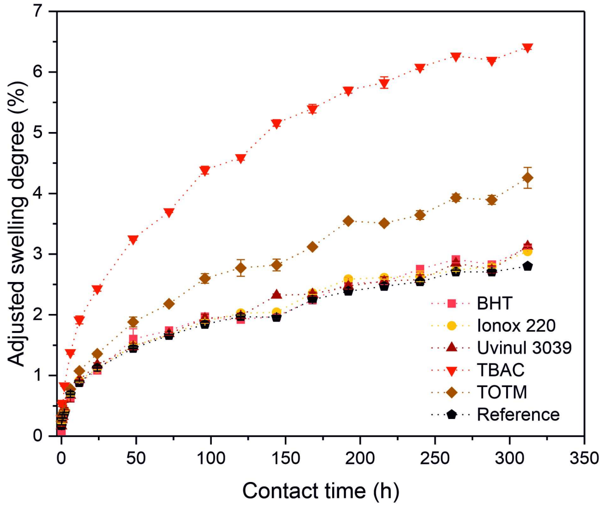
Adjusted swelling degree (%)
Contact time (h)
0
1
2
3
4
5
6
7
0
50
100
150
200
250
300
350
BHT
Ionox 220
Uvinul 3039
TBAC
TOTM
Reference

2.B

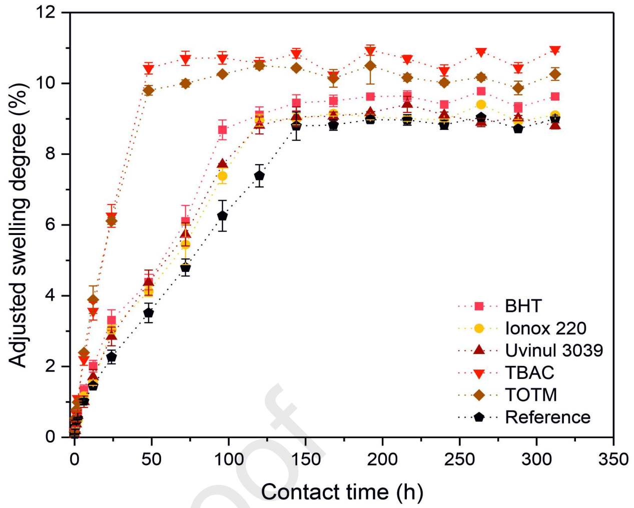
Adjusted swelling degree (%)
Contact time (h)
0
2
4
6
8
10
12
0
50
100
150
200
250
300
350
BHT
Ionox 220
Uvinul 3039
TBAC
TOTM
Reference

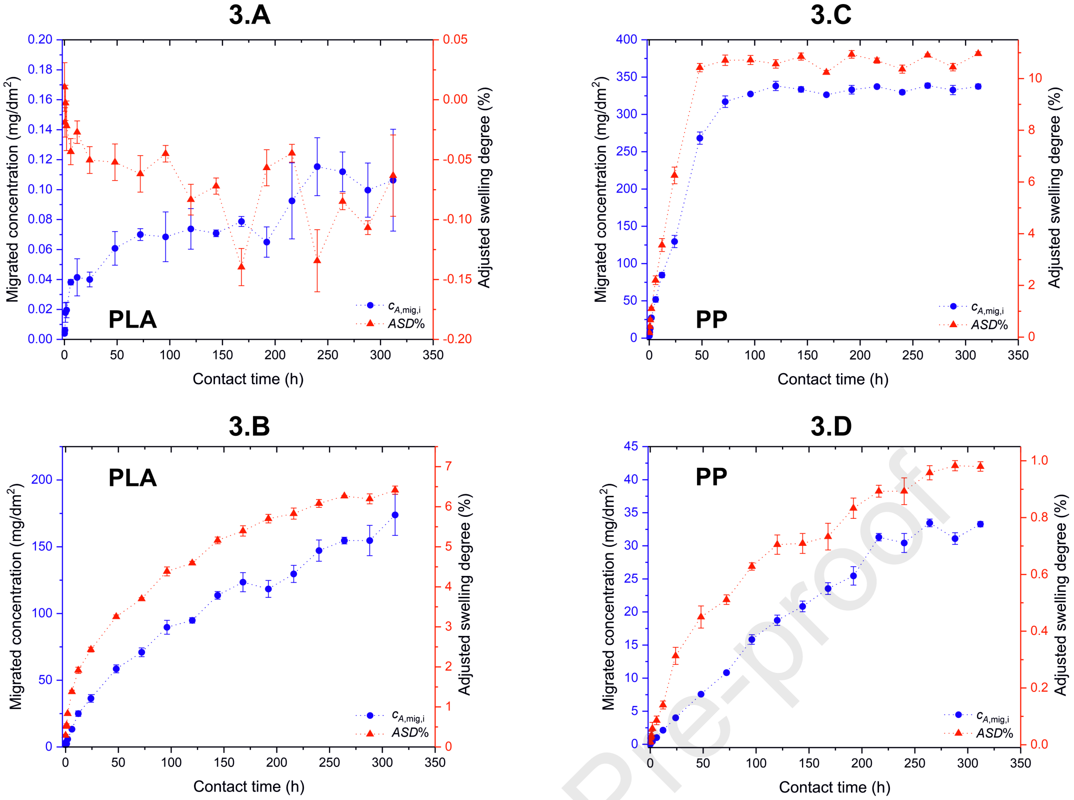
3.A
PLA
Migrated concentration (mg/dm^2)
Adjusted swelling degree (%)
Contact time (h)
0.00
0.02
0.04
0.06
0.08
0.10
0.12
0.14
0.16
0.18
0.20
0.05
0.00
-0.05
-0.10
-0.15
-0.20
0
50
100
150
200
250
300
350
$c_{A,mig,i}$
ASD%
3.C
PP
Migrated concentration (mg/dm^2)
Adjusted swelling degree (%)
Contact time (h)
0
50
100
150
200
250
300
350
400
0
2
4
6
8
10
$c_{A,mig,i}$
ASD%
3.B
PLA
Migrated concentration (mg/dm^2)
Adjusted swelling degree (%)
Contact time (h)
0
50
100
150
200
0
1
2
3
4
5
6
7
$c_{A,mig,i}$
ASD%
3.D
PP
Migrated concentration (mg/dm^2)
Adjusted swelling degree (%)
Contact time (h)
0
5
10
15
20
25
30
35
40
45
0.0
0.2
0.4
0.6
0.8
1.0
$c_{A,mig,i}$
ASD%

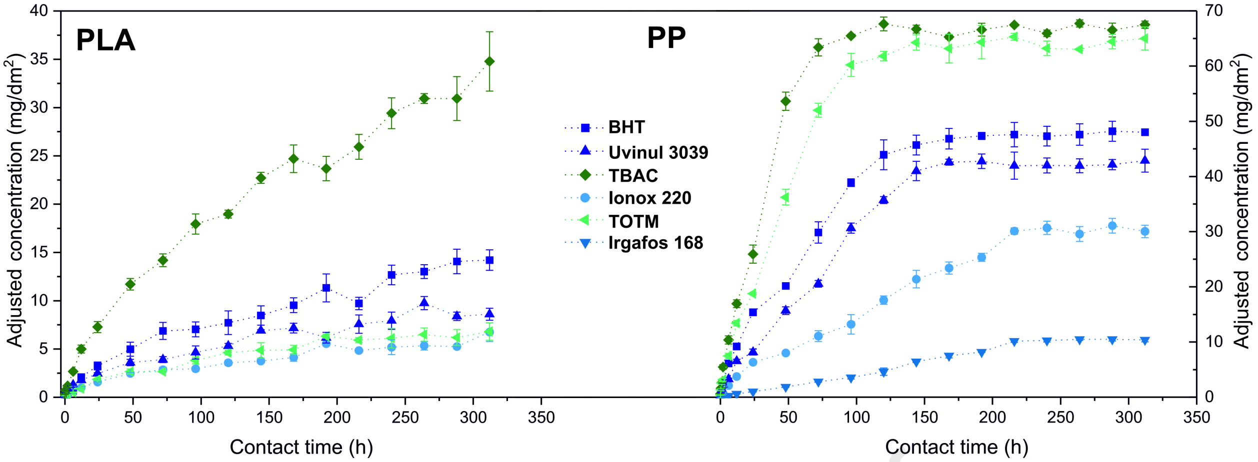
PLA
PP
Adjusted concentration (mg/dm^2)
Contact time (h)
0
5
10
15
20
25
30
35
40
0
50
100
150
200
250
300
350
0
10
20
30
40
50
60
70
BHT
Uvinul 3039
TBAC
Ionox 220
TOTM
Irgafos 168

5.A

PLA – Uvinul 3039 – EtOH

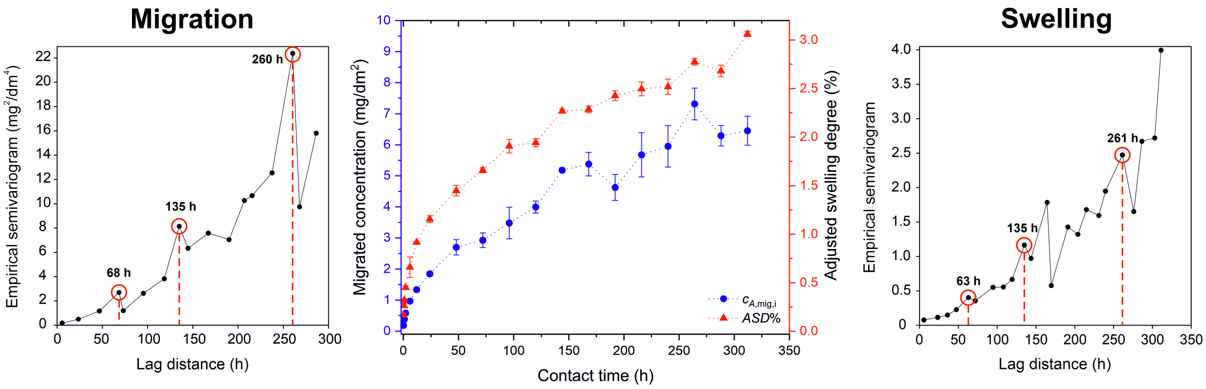

5.B

PP – BHT – EtOH

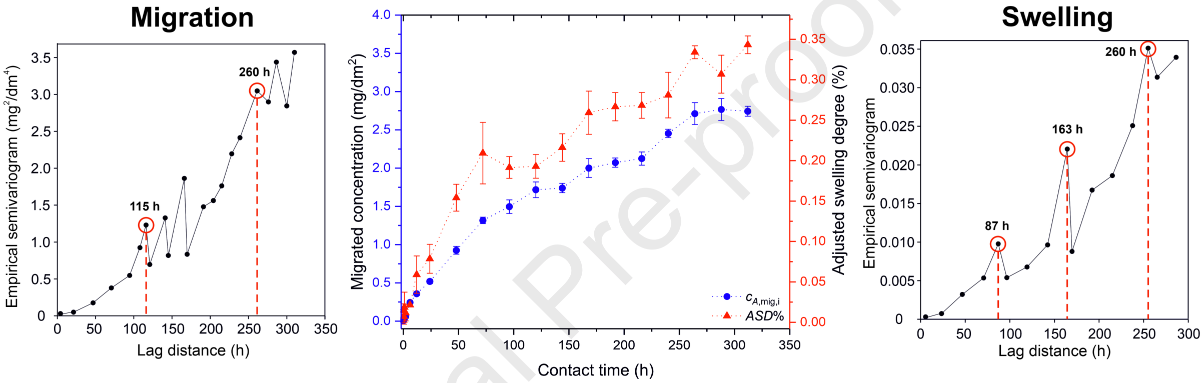

Highlights

- Migration and swelling kinetics of polylactic acid and polypropylene were studied.
- Swelling strongly affects plastic additive migration from food contact materials.
- The effect of molecular weight on additive migration can be overruled by plasticizers.
- Variography was successfully applied to identify steady-states on kinetic curves.

Conflict of interest form

The authors:

Csaba Kirchkeszner[a,b,‡], Noémi Petrovics[a,b, ‡], Tamás Tábi[c,d], Norbert Magyar[e], József Kovács[f], Bálint Sámuel Szabó[a,b], Zoltán Nyiri[b], Zsuzsanna Eke[a,g*]

[a] Hevesy György PhD School of Chemistry, Eötvös Loránd University, Pázmány Péter stny. 1/A, H-1117 Budapest, Hungary

[b] Joint Research and Training Laboratory on Separation Techniques, Institute of Chemistry, Eötvös Loránd University, Pázmány Péter stny. 1/A, H-1117 Budapest, Hungary

[c] Department of Polymer Engineering, Faculty of Mechanical Engineering, Budapest University of Technology and Economics, Műegyetem rkp. 3, H-1111 Budapest, Hungary

[d] MTA-BME Research Group for Composite Science and Technology, Műegyetem rkp. 3, H-1111 Budapest, Hungary

[e] Department of Methodology for Business Analyses, Faculty of Commerce, Hospitality and Tourism, Budapest Business School, Alkotmány u. 9–11, H-1054 Budapest, Hungary

[f] Department of Geology, Institute of Geography and Earth Sciences, Eötvös Loránd University, Pázmány Péter stny. 1/C, H-1117 Budapest, Hungary

[g] Wessling International Research and Educational Center, Anonymus u. 6, H-1045 Budapest, Hungary

* Corresponding author.

‡ These two authors contributed equally to the work.

declare that they have no conflict of interest.